


Examination and modification of Co structures on Ge(001)

Johann Tonhäuser , Nico Kubetschek , Ulrike Kürpick, and René Matzdorf*
Institute of Physics, University of Kassel, Heinrich-Plett-Str. 40, Kassel D-34132, Germany

 (Received 17 February 2022; revised 7 July 2022; accepted 18 August 2022; published 6 September 2022)

High-resolution scanning tunneling microscopy and spectroscopy enlighten the formation and composition of self-organized Co-induced structures on Ge(001). Dimer vacancies due to subsurface Co accumulate and lead to the formation of well-ordered embedded structures which consist of two alternating building blocks. A mismatch in the alternation leads to protrusions at both sides of the structures. The deposition of small amounts of Au changes the internal order of the embedded Co structures and results in longer elongated chains. Supported by Monte Carlo simulations, this modification of chain length is attributed to stress relief due to the insertion of Au-induced dimer vacancies in the Ge(001) surface.

DOI: [10.1103/PhysRevB.106.115404](https://doi.org/10.1103/PhysRevB.106.115404)

I. INTRODUCTION

As microelectronics develops towards the nanometer range, the interest in bottom-up methods has increased [1,2]. Vapor deposition of suitable atoms offers the possibility to create self-organized nanostructures on surfaces consisting of only a few atoms. Metallic nanowires on semiconductors are of particular interest and a fundamental understanding of structural and electronic properties is essential to create nanowires with desired properties. Interestingly, different transition metals on the Ge(001) surface are suitable to form one-dimensional (1D) nanostructures such as iridium (Ir) and cobalt (Co) [3–5] or nanowire arrays, such as gold (Au) and platinum (Pt) [6–9]. Previous works on the system Co/Ge(001) with coverages higher than one monolayer (ML) Co yielded well-shaped three-dimensional clusters [10–12], while much higher coverages of cobalt resulted in thin films [13,14]. The authors showed that the clusters and thin films consist of different compositions of Co_xGe_y . Choi *et al.* deposited small amounts (less than 5% of a ML) of Co on Ge(001) and showed based on scanning tunneling microscopy (STM) measurements and density-functional theory calculations that Co induces dimer vacancies (DVs) caused by Co atoms in the subsurface area, which diffuse along the Ge(001) dimer rows [15]. Zandvliet *et al.* and Grzela *et al.* investigated Co nanostructures after deposition 0.1–0.25 ML Co and postannealing up to 700 K [5,11]. In STM images the structure shows a hexagonal or rectangular arrangement of bright spots, depending on the bias voltage and chains, which are oriented perpendicular to the dimer rows. After heating the samples above 700 K, long exalted nanowires appear, with length of about 100 nm and with two parallel atomic rows on top [5].

A detailed understanding of the development and atomic composition of the self-organized Co-induced nanostructures on Ge(001) is of fundamental as well as technological interest,

because electronic and magnetic properties depend on the atomic structure.

In this work we focus on the initial steps of the formation of Co-induced nanostructures after submonolayer deposition of Co on Ge(001) and explore their detailed structural properties using high-resolution scanning tunneling microscopy (STM) and spectroscopy (STS). We identified two different building blocks, which are the elementary units for longer chains. In a temperature range from 450 to 650 K it has been studied how the structures depend on the annealing temperature. At 650 K embedded nanostructures have formed. Furthermore, we investigate the influence of additionally deposited Au (up to 30% of a ML) on the Co structures.

II. EXPERIMENTAL DETAILS

The experiments were performed under ultrahigh-vacuum conditions at a base pressure of 1.2×10^{-11} mbar. Antimony-doped germanium substrates were used with a specific resistivity between 0.01 and 0.1 Ω cm. The preparation of the clean Ge(001) surface was carried out according to the method of Blumenstein *et al.* [16]. Cobalt was evaporated from an electron beam evaporator and 0.13–0.2 monolayers (area coverage) were deposited on the Ge(001) surface with postannealing at 650 K for 10 min. During the preparation the pressure in the chamber never exceeded 2.0×10^{-9} mbar. For the temperature series the samples were successively annealed for 10 min in the range of 450–650 K. For the modification of the chain lengths Au was evaporated from another electron evaporator and 0.2 ML were additionally deposited on the Co-covered Ge(001) surface and annealed at a temperature of 650 K for an additional 10 min. The STM measurements were performed with a commercial Omicron LT-STM at 5 and 77 K using an electrochemically etched Ag covered tungsten tip, which was tested on a monocrystalline Ag(111) surface before the measurements on the Ge(001) system were performed. The spectra were measured with a standard lock-in technique with a modulation frequency of 900 Hz and an amplitude of $V_{\text{amp}} = 5$ mV.

*matzdorf@physik.uni-kassel.de

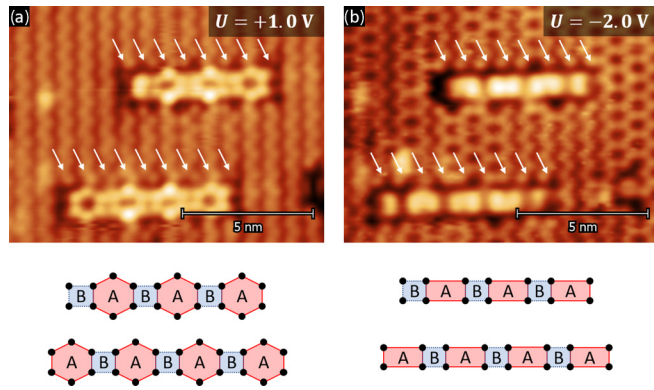


FIG. 1. Empty (a) and filled (b) state STM images of embedded Co structures (a) at sample bias of +1.0 V, (b) at sample bias of -2.0 V; the tunneling current was 0.1 nA. The white arrows indicate the interrupted dimer rows. Below the measured images a schematic drawing of the structures of both embedded chains is shown with the building blocks A (red shaded) and B (blue shaded).

III. RESULTS AND DISCUSSION

A. Structural analysis

After the deposition of Co in the submonolayer regime on the Ge(001) surface and subsequent annealing of the sample, several different structures appear. In addition to several different types of DVs, vacancy islands, and disordered structures, also embedded structures occur, which are geometrically well ordered. Topographies of these well-ordered embedded Co structures measured at negative and positive bias voltages are shown in Figs. 1(a) and 1(b). White arrows indicate interrupted Ge dimer rows. In Fig. 1(a) the embedded Co structures appear to consist of two building blocks denoted as A and B. At positive bias voltage block A is formed by six bright spots in a hexagonal shape and block B is formed by four spots in a rectangular shape with edge lengths of about 0.6 nm. For negative bias voltage both building blocks appear as rectangular-shaped structures with two different lengths of (0.97 ± 0.09) nm (A) and (0.58 ± 0.05) nm (B), as shown in Fig. 1(b). The appearance of the A block at positive and negative bias voltages differs by two spots, which are visible in the empty states and invisible in the occupied states. These spots are denoted as outer spots, while the always visible spots are called inner spots in the following. The B block has the same appearance for positive and negative bias voltages. The length of both building blocks A and B together coincides with every second dimer row of the Ge substrate. A schematic drawing of the configuration is shown below the figures for both embedded structures in detail. We counted around 2500 embedded structures on ten different topographies with an area coverage of 20% cobalt and a total area of $100\,000$ nm². Only 7% of the structures end at one side with a B block; most structures end on both sides with A blocks. We never observed a structure which was terminated at both ends with B blocks. Due to this and the fact that both building blocks exist, it is not possible to describe the complete structures in terms of unit cells, whereas the internal structure can be described by AB unit cells. The interrupted dimer rows are used as a length indicator for the embedded

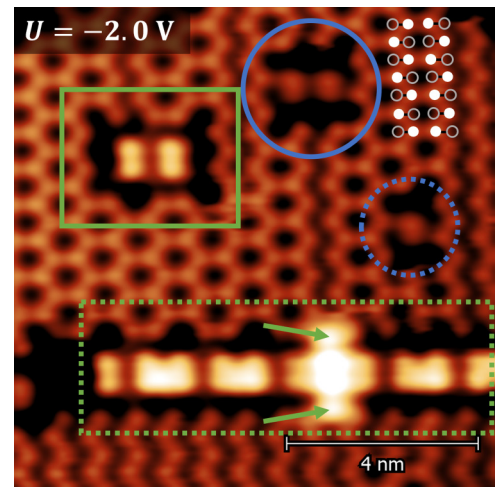


FIG. 2. Filled state STM image of embedded Co structures (green rectangle) and Co-induced DV (blue circles). The green arrows indicate the protrusions of the chain. The sample bias was -2.0 V and the tunnel current was 0.3 nA. Ge dimer rows are indicated by a ball-and-stick model in the upper right corner.

structures. Along the dimer rows the embedded structures interrupt four Ge dimers per row, while perpendicular to the dimer rows it depends on the number of A and B building blocks as

$$D_{\text{rows}} = 2 + n_A + n_B, \quad (1)$$

where n_A and n_B are the numbers of A and B blocks, respectively, and D_{rows} denotes the number of interrupted dimer rows. The Ge dimer rows in Fig. 1(a) exhibit a $p(2 \times 2)$ reconstruction, where the dimers of adjacent rows buckle in phase, while the dimers in Fig. 1(b) mainly show a $c(4 \times 2)$ reconstruction, where the dimers of neighboring rows buckle in opposite directions. The predominant reconstruction of the Ge(001) surface depends on the bias voltage, as reported by Takagi *et al.* [17]. To guide the eye, the interrupted dimer rows in Fig. 1 are marked with white arrows. In Figs. 2 and 4 respective dimer rows are indicated by ball-and-stick models, where the white balls indicate the up-buckled atoms of the respective dimers, which are visible in the STM images and

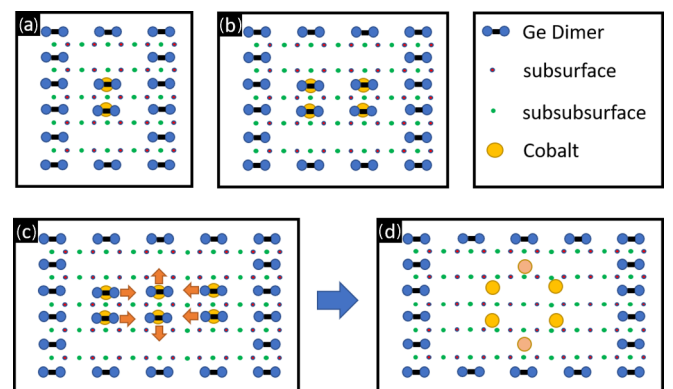


FIG. 3. Models for a (1++1) DV (a) and a $2 \times (1++1)$ DV (b). Three (1++1) DVs in alignment transform immediately to a hexagonal A block (c) \rightarrow (d).

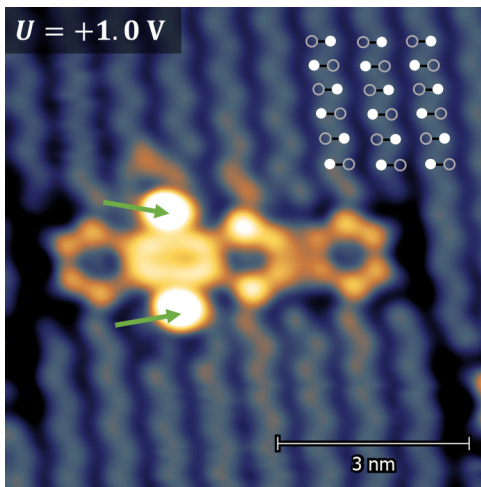


FIG. 4. Empty state STM image of an embedded Co structure with protrusions (green arrows). The sample bias was +1.0 V and the tunnel current was 0.4 nA. Ge dimer rows are indicated by a ball-and-stick model in the upper right corner.

the unfilled balls indicate the down-buckled atoms. In Fig. 2 the ball-and-stick model marks dimers in the $c(4 \times 2)$ reconstruction and in Fig. 4 the indicated dimers show the $p(2 \times 2)$ reconstruction. Two types of Co-induced DVs, a single A building block and a longer embedded Co structure, are shown in Fig. 2. A single $(1++1)$ DV is marked with a blue dotted circle. A double DV is marked with a closed blue circle and is denoted as $2 \times (1++1)$ DV. This denotation was taken over from Choi *et al.* [15]. The single and double DVs are aligned in phase with the dimer rows and appear as two close-lying dots between two vacancies along the dimer row. A single block A, of which the outer spots are not visible in the topography measured with negative bias voltage, is shown in the green closed lined rectangle. Unlike the $2 \times (1++1)$ DVs, only these invisible outer spots are in phase with a dimer row, while the inner spots are placed between two dimer rows. These out-of-phase spots are a reliable feature to distinguish between $2 \times (1++1)$ DVs and blocks A.

Interestingly, we never observed a $3 \times (1++1)$ DV perfectly aligned to each other. In Fig. 3(c) a model is suggested, how DVs are composed and how A blocks are built on the basis of DVs. In agreement with Choi *et al.* we assume that Co is positioned under the dots in the subsurface region [15]. In Fig. 3(a) a single $(1++1)$ DV is shown. Due to diffusion of single DVs, double $2 \times (1++1)$ DVs are created. We assume that as soon as a third $(1++1)$ DV joins a $2 \times (1++1)$ DV the atoms rearrange immediately to an A block as indicated in Figs. 3(c) \rightarrow 3(d). Within this model the A blocks consist of six Co atoms arranged in a hexagon, in agreement with a suggestion of Zandvliet *et al.* [5]. Since the Co atoms are located in the subsurface the observed structures are referred to as embedded. Depending on the bias voltage, the structures in the STM images have an apparent height of roughly about 40% (≈ 55 pm) of a monolayer from Ge(001). However, STM images arise due to topographic features combined with contributions from the local density of states, so the true height of the structures remains unknown. In Fig. 2, an embedded Co structure, which shows protrusions, is marked by a green

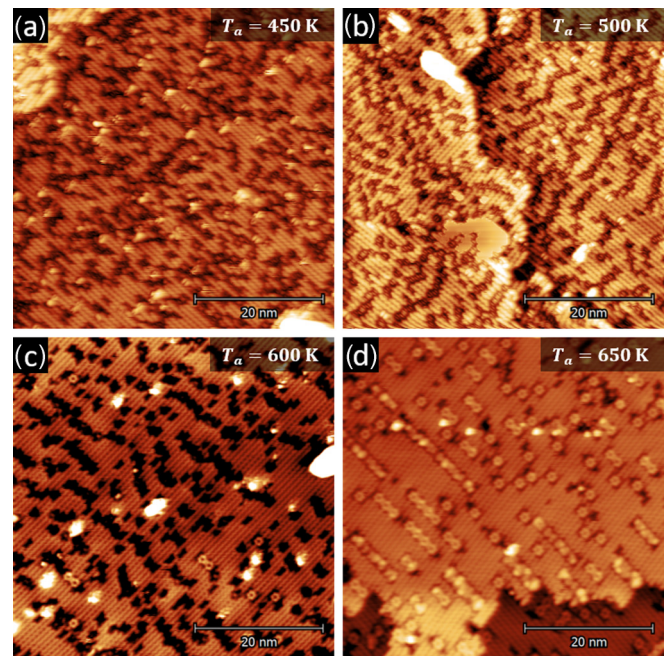


FIG. 5. Empty state STM images measured at $T = 77$ K after different annealing temperatures with a coverage of 0.2 ML cobalt: (a) $T_a = (450 \pm 50)$ K, (b) $T_a = (500 \pm 50)$ K, (c) $T_a = (600 \pm 50)$ K, and (d) $T_a = (650 \pm 50)$ K. The sample bias was +1.0 V and the tunnel current was 0.2 nA.

dotted rectangle. The protrusions are indicated by green arrows. It seems that a deviation in the sequence of alternating A and B blocks leads to a mismatch with the Ge(001) substrate dimer rows, causing these protrusions. In Fig. 4 protrusions are shown in another structure in a STM image of unoccupied states. The protrusions are exactly in between two dimer rows. The small rectangle, which becomes visible between the protrusions, is about 1.2 nm in length. Equation (1) yields eight interrupted dimer rows for an ABBABA structure, in agreement with the measurement. Thus we assume that a sequence of two consecutive B blocks causes the protrusions.

The dependence of Co-induced structures on Ge(001) on the annealing temperature is investigated by a series of annealing temperatures in the range from (450–650) K. In Fig. 5 topographies measured after annealing temperatures of 450 K (a), 500 K (b), 600 K (c), and 650 K (d) are shown. After annealing at 450 K many adatoms and DVs are present on the surface. A slight increase of the annealing temperature to 500 K reduces the amount of adatoms and leads to an arrangement of the DVs in chains, which are roughly perpendicular to the dimer rows. However, it should be noted that chains of DVs are not strictly linear. The first hexagonal structures appear at an annealing temperature of 600 K. At about 650 K nearly all DVs are vanished and many single A blocks as well as straight chains composed of alternating A and B blocks are visible. Besides these well-ordered structures, also longer chains appear, which are disordered. Despite the similarity of clean (001) surfaces of Si and Ge, the two surfaces exhibit differences in terms of vacancies. The formation energy of single DVs is significantly higher on Ge than on Si and self-organized dimer vacancy lines appear only

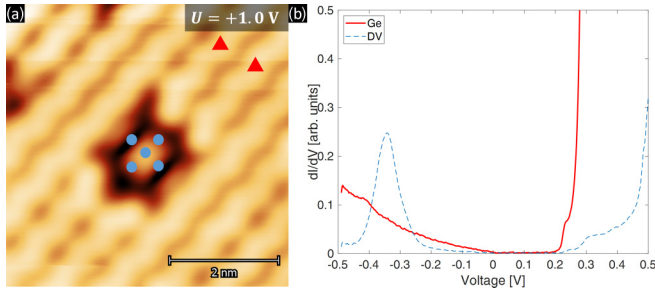


FIG. 6. (a) Empty state STM image of a $2 \times (1++1)$ DV on Ge(001). Spectra locations are marked with triangles (red) and dots (blue). (b) The STS spectra were recorded with a lock-in amplifier at LHe temperature. The set point for the spectra was $U = -0.5$ V and $I = 0.3$ nA.

on the Si(001) surface but not on clean Ge(001) [18]. The deposition of Co or Ni on Si(001) leads to quite regularly arranged impurity-induced dimer vacancy lines and the surfaces reconstruct showing a $(2 \times n)$ periodicity with n between 6 and 9 [19,20]. The chains of dimer vacancies in Figs. 5(b) and 5(c) are shorter and less regular than the impurity-induced lines on Si(001); nevertheless, similarly to the lines on Si, they are built from Co-induced DVs.

According to the model in Fig. 3, the A blocks are built instantaneously from three strictly aligned $(1++1)$ DVs. The slightly bent chains of DVs in Fig. 5(c) cover about 27% of the surface and the A blocks and straight chains of alternating A and B blocks in Fig. 5(d) cover about 20% of the surface. Since we never observed adsorbed Ge dimers or adsorbed dimer chains on the surface, we consider it likely that the displaced Ge dimers fill up remaining vacancies near the ordered structures during the transformation step in Figs. 3(c) to 3(d) or reach step edges. The results obtained after different annealing temperatures support the model proposed in Fig. 3.

B. Spectroscopic features

Density of states (DOS) of DVs and well-ordered embedded Co structures are measured to reveal their electronic properties. A topography of a $2 \times (1++1)$ DV on Ge(001) is exhibited in Fig. 6(a), in which the locations where spectra were recorded are marked with blue dots. The respective spectra are shown in Fig. 6(b) in comparison with spectra taken from the Ge(001) surface. The DOS signal of the $2 \times (1++1)$ DV reveals a significant peak at a bias voltage of about -0.35 V as shown in Fig. 6 (blue dashed curve), while the Ge spectra (red solid line) are in good agreement with the band gap of 0.25 eV [21,22]. Himpsel *et al.* [23] measured a d -like bulk state at -0.35 eV and a surface state at -0.3 eV on Co(0001) using angle-resolved photoemission. Peaks between -0.31 and -0.5 eV have been reported by Diekhöner *et al.* [24], Mocking *et al.* [12], Barral *et al.* [25], and Eom *et al.* [26], for Co islands [12,24] and films [25] on different substrates or for clean Co(0001) surfaces [25,26]. According to these results, we associate the peak at -0.35 eV to the presence of Co atoms, which further supports the model [Fig. 3(b)].

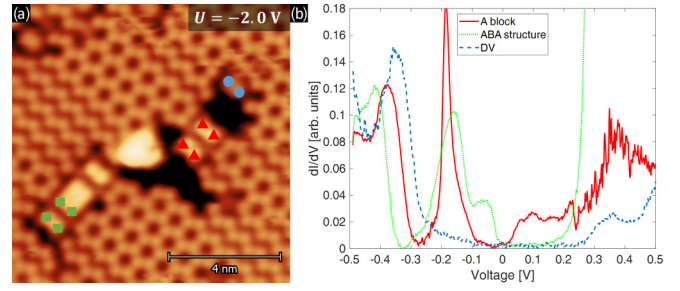


FIG. 7. (a) Filled state STM image of Co embedded structures on Ge(001). Spectra locations are marked with triangles (red), dots (blue), and rectangles (green). (b) The STS spectra were recorded with a lock-in amplifier at LHe temperature. The set point for the spectra was $U = -0.5$ V and $I = 0.3$ nA.

Furthermore, spectra were measured on embedded well-ordered Co structures as shown in Fig. 7. A topography is shown in Fig. 7(a) in which locations where spectra were measured are marked by green rectangles (ABA Co structure), red triangles (single A block), and blue dots (DV). The respective spectra are shown in Fig. 7(b). It is interesting to note that all spectra have a peak between -0.35 and -0.42 V which we consider to be a characteristic sign for Co. In addition, both embedded structures show a peak at about -0.19 V. An additional peak at -0.2 eV has been reported by Muzychenko *et al.* [27] measured on Co/Ge(111) $\sqrt{13} \times \sqrt{13} R13.9^\circ$ reconstructed nanoislands, which consist of mixed Co and Ge atoms. The authors associated this surface state with a different contribution of the Co and Ge atoms. We interpret the measured peak at -0.19 eV to be a sign for a Co-Ge bond.

C. Modification of chain length

The length distribution of the well-ordered structures, which are composed of alternating A and B blocks, is determined from ten STM topographies with a total area of 100.000 nm². The length L corresponds to the amount of A blocks in an ideal alternating A and B block chain, i.e., length 1 is a single A block, length 2 is an ABA chain, and so on. For nonalternating chains, the length L was determined using Eq. (1) via the number of interrupted Ge(001) dimer rows. The measured length distribution is compared to results from Monte Carlo (MC) simulations by using the Metropolis MC algorithm [28]. We modified the algorithm using an attractive effective pair interaction (EPI) in one direction and an equally strong repulsive interaction in the other direction to get anisotropic structures.

In Fig. 8 the distributions are shown for the measurement (gray bar), the simulated data with an EPI of 60 meV (black bar), and the random case with an EPI of 0 meV (white bar). The best EPI of 60 meV was found with the method of least squares.

A comparison of the measured and the simulated data reveals that the Co structures are not randomly distributed. The simulation with an EPI = 60 meV fits the data quite well for small chain lengths but overestimates longer chains. This discrepancy might be explained by stress due to a slight mismatch between the Ge dimer rows and the embedded Co structures. The stress increases with increasing chain length

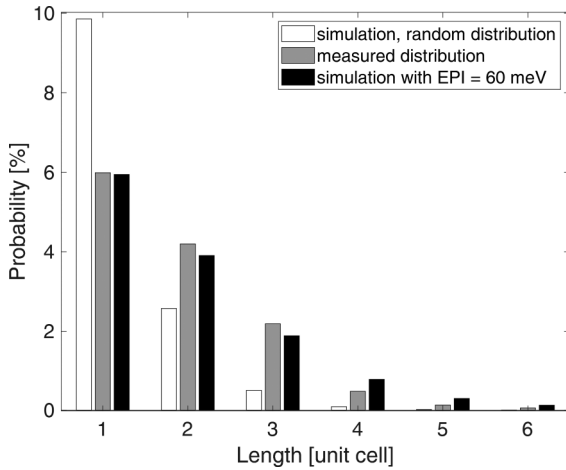


FIG. 8. Length distributions of embedded Co structures with a coverage of about 13%. Gray bars show the measured distribution, white and black bars represent the simulated distributions for an EPI = 0 meV (white) and an EPI = 60 meV (black), and a freeze temperature $T_{\text{freeze}} = 500$ K.

and counteracts the growth of longer well-ordered chains. This interpretation is also consistent with the observation that longer chains appear to be disordered, as shown in Fig. 5(d).

Many *d*-block metals in the low coverage regime induce DVs on Ge(001) [13,29,30]. Therefore, we deposited small amounts of Au (e.g., 30% of a ML) to reduce the stiffness of the Ge(001) dimer lattice by the DVs. Topographies in Fig. 9 exhibit a Ge(001) surface which is disturbed by many DVs due to the Au deposition. The additionally deposited Au induces DVs, resulting in a kind of Au/Ge(001) mixed phase [29]. The longest well-ordered embedded Co structures on the surface are marked in Fig. 9(a) with black arrows. They are significantly longer than the structures on the pure Ge(001) surface. Interestingly, the internal structure has changed too. The chains consist partly of successive A blocks instead of alternating A and B blocks, as highlighted in Fig. 9(b) by the blue circle. The well-known (1 + 2 + 1) DVs [29] of the

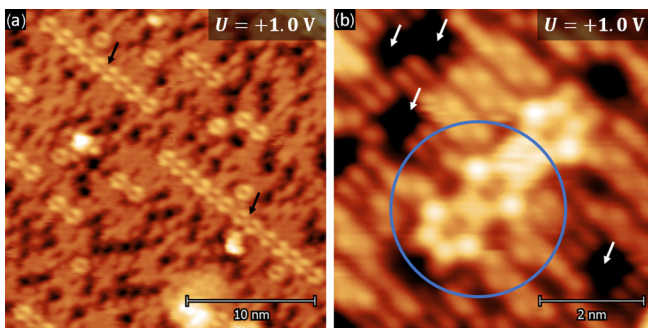


FIG. 9. Empty state STM image of Co embedded structures on Ge(001) with an additional Au coverage of 30%. (a) Elongated Co structures marked with black arrows and sequences of AAAAAAAAAABA (upper chain) and AAAAAABAABAAAABA (lower chain). (b) High resolved AABA structure. The blue circle indicates the AA structure and the white arrows mark the gold-induced DVs on Ge(001).

TABLE I. Measured length distributions of embedded Co structures grown on a clean Ge(001) surface and after additional Au deposition. The total area coverage of well-ordered Co structures is 20% before and 22.5% after Au deposition.

Length L	Co coverage	Co coverage with Au mod.	Change (%)
1	0.1068	0.0883	-17
2	0.0534	0.0612	+15
3	0.0204	0.0448	+119
4	0.0104	0.0193	+86
5	0.0035	0.0067	+91
6	0.0015	0.0031	+101
7	0.0006	0.0018	+200
Σ	0.1968	0.2253	+14.5

mixed Au phase are marked with white arrows. Moreover, we no longer recognize disordered embedded Co structures like in Fig. 5(d).

For a quantitative comparison between Co structures on pure Ge(001) and on Ge(001), which was modified with Au, we counted embedded Co structures with a total area of about 40.000 nm². The total area coverage of well-ordered Co structures on the surface before Au deposition was 20% and after Au modification the area coverage of the well-ordered Co structures increases up to 22.5%. The results are summarized in Table I.

The amount of structures with the length 1 decreases, while the numbers of all other chains increase. The amount of chains with $L = 2$ increases by about 15%. For chains with $L = 3$ up to $L = 6$, the total coverage approximately doubles. The higher increase of 200% for chains with $L = 7$ is probably due to statistics, since the absolute numbers here are one chain and three chains, respectively. The significant increase of the numbers of structures with longer length after deposition of Au provides further support for the interpretation, that the length of the well-ordered structures is limited by stress, because the stress of the rigid Ge lattice has been reduced by implemented Au DVs. The total amount of Co embedded structures increases by 14.5%. We attribute this to the fact that the disordered structures which appear only on the pure Ge substrate were previously not taken into account. They may have transformed into well-ordered structures.

IV. CONCLUSION

We have shown that vapor-deposited cobalt in the sub-monolayer range on a Ge(001) surface induces dimers vacancies and well-ordered embedded nanostructures. The structures consist of two different and alternating building blocks A and B. The center axis of each building block A is in phase with every second substrate dimer row, just like the center axis of blocks B. In the case that this periodicity is interrupted by two successive B blocks, two opposite protrusions appear in the STM image, located laterally to the longitudinal axis of the embedded structures and between two rows of substrate dimers. Furthermore, we show that the embedded structures are significantly extended by the insertion of

gold-induced DVs and their strict alternation of A and B blocks has vanished, thus providing a possibility to manipulate the growth of self-organized structures. STS spectra reveal two states at 0.35 and 0.19 eV below the Fermi level.

The former is attributed to a Co peak, and the latter is associated with the embedded Co structures. We provide further evidence that the DVs are due to cobalt in the subsurface and that the A blocks probably consist of six cobalt atoms.

-
- [1] S. B. Desay, S. R. Madhupathy, and A. B. Sachid, MoS₂ transistors with 1-nanometer gate length, *Science* **354**, 99 (2016).
- [2] N. A. Melosh, A. Boukai, F. Diana, B. Gerardot, A. Badolato, P. M. Petroff, and J. R. Heath, Ultrahigh-density nanowire lattices and circuits, *Science* **300**, 112 (2003).
- [3] N. S. Kabanov, R. Heimbuch, H. Zandvliet, A. M. Saletsky, and A. L. Klavsyuk, Atomic structure of self-organizing iridium induced nanowires on Ge(001), *Appl. Surf. Sci.* **404**, 12 (2017).
- [4] T. F. Mocking, P. Bampoulis, N. Oncel, B. Poelsema, and H. J. W. Zandvliet, Electronically stabilized nanowire growth, *Nat. Commun.* **4**, 2387 (2013).
- [5] H. J. Zandvliet, A. van Houselt, and P. E. Hegeman, Embedded Co islands on Ge(001), *Surf. Sci.* **605**, 1129 (2011).
- [6] C. Blumenstein, J. Schäfer, S. Mietke, S. Meyer, A. Dollinger, M. Lochner, X. Y. Cui, L. Patthey, R. Matzdorf, and R. Claessen, Atomically controlled quantum chains hosting a Tomonaga–Luttinger liquid, *Nat. Phys.* **7**, 776 (2011).
- [7] J. Schäfer, C. Blumenstein, S. Meyer, M. Wisniewski, and R. Claessen, New Model System for a One-Dimensional Electron Liquid: Self-Organized Atomic Gold Chains on Ge(001), *Phys. Rev. Lett.* **101**, 236802 (2008).
- [8] M. Fischer, A. van Houselt, D. Kockmann, B. Poelsema, and H. J. W. Zandvliet, Formation of atomic Pt chains on Ge(001) studied by scanning tunneling microscopy, *Phys. Rev. B* **76**, 245429 (2007).
- [9] A. van Houselt, T. Gnielka, J. M. Aan de Brugh, N. Oncel, D. Kockmann, R. Heid, K.-P. Bohnen, B. Poelsema, and H. J. Zandvliet, Peierls instability in Pt chains on Ge(001), *Surf. Sci.* **602**, 1731 (2008).
- [10] K. Sell, A. Kleibert, V. V. Oeynhausen, and K.-H. Meiwes-Broer, The structure of cobalt nanoparticles on Ge(001), *Eur. Phys. J. D* **45**, 433 (2007).
- [11] T. Grzela, W. Koczorowski, G. Capellini, R. Czajka, M. W. Radny, N. Curson, S. R. Schofield, M. A. Schubert, and T. Schroeder, Interface and nanostructure evolution of cobalt germanides on Ge(001), *J. Appl. Phys.* **115**, 074307 (2014).
- [12] T. F. Mocking, G. Hlawacek, and H. Zandvliet, Cobalt induced nanocrystals on Ge(001), *Surf. Sci.* **606**, 924 (2012).
- [13] J. Choi, D. K. Lim, Y. Kim, and S. Kim, Structural and electronic properties of cobalt germanide islands on Ge(100), *J. Phys. Chem. C* **114**, 8992 (2010).
- [14] K. De Keyser, R. L. Van Meirhaeghe, C. Detavernier, J. Jordan-Sweet, and C. Lavoie, Texture of cobalt germanides on Ge(100) and Ge(111) and its influence on the formation temperature, *J. Electrochem. Soc.* **157**, H395 (2010).
- [15] J. Choi, D. K. Lim, Y. Kim, D. H. Kim, and S. Kim, Creation and annihilation of single atom vacancy during subsurface diffusion, *Phys. Rev. B* **82**, 201305 (2010).
- [16] C. Blumenstein, S. Meyer, S. Ruff, B. Schmid, J. Schaefer, and R. Claessen, High purity chemical etching and thermal passivation process for Ge(001) as nanostructure template, *J. Chem. Phys.* **135**, 064201 (2011).
- [17] Y. Takagi, Y. Yoshimoto, K. Nakatsuji, and F. Komori, Local and reversible change of the reconstruction on Ge(001) surface between $c(4\times 2)$ and $p(2\times 2)$ by scanning tunneling microscopy, *J. Phys. Soc. Jpn.* **72**, 2425 (2003).
- [18] C. V. Ciobanu, D. T. Tambe, and V. B. Shenoy, Comparative study of dimer-vacancies and dimer-vacancy lines on Si(001) and Ge(001), *Surf. Sci.* **556**, 171 (2004).
- [19] V. Scheuch, B. Voigtländer, and H. Bonzel, Nucleation and growth of CoSi₂ on Si(100) studied by scanning tunneling microscopy, *Surf. Sci.* **372**, 71 (1997).
- [20] M. Kuzmin, J.-P. Lehtiö, Z. Rad, J. Mäkelä, A. Lahti, M. Punkkinen, P. Laukkanen, and K. Kokko, Dimer-vacancy defects on Si(1 0 0): The role of nickel impurity, *Appl. Surf. Sci.* **506**, 144647 (2020).
- [21] K.-L. Jonas, V. von Oeynhausen, J. Bansmann, and K.-H. Meiwes-Broer, Tunnelling spectroscopy on silver islands and large deposited silver clusters on Ge(001), *Appl. Phys. A* **82**, 131 (2006).
- [22] M. Kolmer, S. Godlewski, H. Kawai, B. Such, F. Krok, M. Saeys, C. Joachim, and M. Szymanski, Electronic properties of STM-constructed dangling-bond dimer lines on a Ge(001)-(2×1):H surface, *Phys. Rev. B* **86**, 125307 (2012).
- [23] F. J. Himpsel and D. E. Eastman, Intrinsic Λ_1 -symmetry surface state on Co(0001), *Phys. Rev. B* **20**, 3217 (1979).
- [24] L. Diekhöner, M. A. Schneider, A. N. Baranov, V. S. Stepanyuk, P. Bruno, and K. Kern, Surface States of Cobalt Nanoislands on Cu(111), *Phys. Rev. Lett.* **90**, 236801 (2003).
- [25] M. A. Barral, M. Weissmann, and A. M. Llois, Characterization of the surface states of Co(0001), Co(111), and ultrathin films of Co on Cu(111), *Phys. Rev. B* **72**, 125433 (2005).
- [26] D. Eom, D. Prezzi, K. T. Rim, H. Zhou, M. Lefenfeld, S. Xiao, C. Nuckolls, M. S. Hybertsen, T. F. Heinz, and G. W. Flynn, Structure and electronic properties of graphene nanoislands on Co(0001), *Nano Lett.* **9**, 2844 (2009).
- [27] D. A. Muzychenko, K. Schouteden, and C. Van Haesendonck, Electronic and atomic structure of Co/Ge nanoislands on the Ge(111) surface, *Phys. Rev. B* **88**, 195436 (2013).
- [28] N. Metropolis, A. W. Rosenbluth, M. N. Rosenbluth, A. H. Teller, and E. Teller, Equation of state calculations by fast computing machines, *J. Chem. Phys.* **21**, 1087 (1953).
- [29] J. Wang, M. Li, and E. I. Altman, Scanning tunneling microscopy study of self-organized Au atomic chain growth on Ge(001), *Phys. Rev. B* **70**, 233312 (2004).
- [30] J. Wang, M. Li, and E. I. Altman, Scanning tunneling microscopy study of Au growth on Ge(001): Bulk migration, self-organization, and clustering, *Surf. Sci.* **596**, 126 (2005).